Available online at www.sciencedirect.com
SCIENCE DIRECT
ELSEVIER
Journal of the European Ceramic Society 26 (2006) 2511–2517
ECERS
www.elsevier.com/locate/jeurceramsoc

Sinter-crystallisation in the diopside–albite system Part I. Formation of induced crystallisation porosity

Alexander Karamanov *, Mario Pelino

Department of Chemical Engineering and Materials, University of L'Aquila, Monteluco di Roio 67100, Italy

Received 8 April 2005; received in revised form 21 June 2005; accepted 26 June 2005
Available online 16 September 2005

Abstract

The sinter-crystallisation was investigated in three model glasses (**G1**, **G2** and **G3**) belonging to the diopside–albite system and forming between 30 and 60% diopside, respectively. The effect of bulk crystallisation on the sintering was studied by the addition of 0.7 wt.% Cr_2O_3 as nucleating agent to the **G2** glass.

The degree of sintering was evaluated by the variation of the apparent density while the crystallisation, by the increasing of the absolute density. The structure and morphology of the sintered glass-ceramics was observed by SEM-BSE.

The results highlighted that the densification is not influenced by the variation of the composition among the three glasses but is inhibited by the diopide formation in **G2-Cr** where bulk nucleation takes place. It was shown that, due to the volume variation related to the diopside crystallisation, a spherical intragranular pores were formed in the glass-ceramics. The amounts of this porosity, named induced crystallisation porosity, increased as function of the crystallisation trend.

Keywords: Sintering; Porosity; Glass-ceramics; Crystallisation; Diopside; Albite

1. Introduction

The sinter-crystallisation is considered as an alternative technology for the glass-ceramics manufacturing, expanding the application range of these materials. By this technique small samples with complicated shape (as dental glass-ceramics[1,2]) may be obtained using fine powders, while very large samples (tiles with size up to 1–1.5 m^2) are produced[1–4] with coarse glass frit. Moreover, the glass-ceramics coating and solders, as well as the composite and fibre reinforced glass-ceramics may be considered as particular applications of sinter-crystallisation.

During the sinter-crystallisation, the densification and the crystalline phase formation take place in the same temperature interval. When the crystallisation trend is low, the sintering is completed before the beginning of the crystalline phase formation, so that its kinetics may be explained by the existing theories of viscous flow sintering.[5–10] In the major part of the sintered glass-ceramics, however, the densification and the crystalline phase formation take place simultaneously and, as a result, the crystallisation reduces or even hinders the sintering rate.

Since the crystallisation starts on the surface, some authors assume that the sintering rate is proportional to the grain surface free of crystals and proposed the following modification of the Frenkel's equation[11–13]:

$$\frac{\Delta L}{\mathrm{Lo}} = \frac{3\sigma}{8R\eta(T)} t[1 - x_s(t)] \quad (1)$$

where ΔL/Lo is the shrinkage, σ is the surface tension, $\eta(T)$ is the viscosity, t is the time and x_s (t) is the surface fraction, covered by the crystal phase.

This relation was used to explain the sintering of stoichiometric cordierite glass powders when, during the heat-treatment, all the grain surface is covered by crystals, i.e. $[1 - x_s\ (t)]$ becomes zero.[12] This model may also be applied

* Corresponding author. Tel.: +39 862 434233; fax: +39 862 434233.
E-mail address: karama@ing.univaq.it (A. Karamanov).

0955-2219/$ – see front matter © 2005 Elsevier Ltd. All rights reserved.
doi:10.1016/j.jeurceramsoc.2005.06.042

to the case of very fine powders or when the sintering particles become rigid due to complete surface crystallisation; it however cannot described all cases of sinter-crystallisation.

According to Eq. (1), a fully sintered material is always obtained when $[1 - x_s\ (t)] > 0$. If, for example, one third of the surface remains amorphous the densification rate must decrease three times. This means that the hindering effect due to crystallisation must be compensated by a 10–20 °C increasing of the temperature (i.e. the temperature difference corresponding to three times lower viscosity). However, the experimental results are somehow different suggesting that a complete model of the sinter-crystallisation must discuss not only the surface crystallisation, but also the changes taking place in the bulk of the grains.

Assuming that the crystalline phase formation increases the apparent viscosity, it was proposed to substitute the parent viscosity of the melt, η, in Eq. (1) with the apparent (effective) viscosity, η_a[14,15]:

$$\frac{\Delta L}{\mathrm{Lo}} = \frac{3\sigma}{8R\eta\{1 + b[P(t)]^n\}} t[1 - x_s(t)] \quad (2)$$

Here η_a is evaluated by the relation: $\eta_a = \eta(1 + bP)^n$; where P is the percentage of crystal phase formed and b and n are constants, higher than 0.025 and 1, respectively.

Since η_a depends on many factors (i.e. the parent viscosity, the nature of the liquid, the size and form of the solid particles and their distribution, etc.) it is described by several empirical relations and theoretical models.[16–18] All relations however predict a rapid increasing of the apparent viscosity after the formation of a "critical" percentage of crystalline phase. Applying these models to the sinter-crystallisation means that sintering to theoretical densification can be obtained only if completed before the formation of the "critical" percentage of crystalline phase; otherwise it will be inhibited by the increasing of the apparent viscosity.

Due to liquid–liquid separation or bulk crystallisation, η_a in the glass forming melts may increase significantly, reaching values 10^4–10^6 higher than the initial shear viscosity of the parent glass. This phenomenon is well known in the production technology of glass-ceramics because it avoids the deformation during the crystallisation heat-treatment.[1,2]

Another peculiarity of the sinter-crystallisation process is the volume variation accompanying the crystalline phase formation,[12,13,19,20] which yields to a shrinkage when the apparent viscosity remains low, or to the formation of additional porosity when η_a becomes high. This last phenomenon is yet not clearly highlighted and investigated.

In the present study, the sinter-crystallisation is investigated by using model glasses, belonging to the albite–diopside phase diagram and forming between 30 and 60% crystal phase. This pseudo-binary system was selected because of several features:

- Diopside is the only crystal phase formed, while the residual glass retains a composition similar to albite.[21]
- The viscosity versus temperature curves of the investigated compositions, evaluated by the Lakatos method, are very similar,[22] which justify the evaluation of the results as a only function of the crystallisation trend.
- The formation of diopside is associated to a high volume variation.[23,24] As a result, in absence of nucleating agents, diopside is formed by surface crystallisation,[25] while by adding small amount of Cr_2O_3 a consistent bulk nucleation and crystallisation is attained.[26–28]

The evolution of the porosity during sintering was investigated by density measurements and related to the surface or bulk mechanism of crystal phase formation. The sintering and crystallisation kinetics were also investigated and will be presented in the second part of this work.

2. Experimental

The theoretical compositions of the investigated three glasses (labelled **G1**, **G2** and **G3**) are reported in Table 1. In order to study the effect of bulk nucleation on the sinter-crystallisation, a 0.3 mol% (0.7 wt.%) Cr_2O_3 was added to **G2**, thus obtaining **G2-Cr** composition. The melting procedure, the experimental results for the glass compositions obtained by XFR analysis and the experimental conditions used to prepare different glass fractions are reported in a previous paper.[22]

In the present study, glass fractions between 75 and 125 μm were used. "Green" samples with initial sizes 10 mm × 10 mm × 8 mm were prepared by mixing the glass powders with 7.5% poly-vinyl alcohol (PVA) solution and by pressing at 100 MPa. After drying and holding at 270 °C (to remove the PVA), the samples were heated to different temperatures in the range 650–1000 °C at a heating rate of 5 and 20 °C/min, sintered for 1 h and cooled at 10 °C/min.

The degree of sintering was evaluated by the variation of the total, P_T, and closed porosity, P_C (by measuring the apparent density, ρ_a, skeleton density, ρ_s, and absolute density of the glass-ceramics samples, ρ_{gc}) through the following relations:

$$P_T = 100\frac{\rho_{gc} - \rho_a}{\rho_{gc}} \quad (3)$$

$$P_C = 100\frac{\rho_{gc} - \rho_S}{\rho_{gc}} \quad (4)$$

Table 1
Chemical compositions of the studied glasses (mol%)

	G1	G2	G2-Cr	G3
SiO_2	54	58	58	62
Al_2O_3	2	4	4	6
Cr_2O_3	–	–	0.3	–
CaO	21	17	17	13
MgO	21	17	17	13
Na_2O	2	4	4	6

where ρ_a was measured by a dry flow pycnometer (GeoPyc 1360), ρ_s and ρ_{gc} – by He displacement Pycnometer (AccuPyc 1330). First skeleton density was measured and then the absolute density after crashing and milling the samples below 40 μm. The experimental associated errors to the evaluation of ρ_a, ρ_{gc} and ρ_s were estimated as ±0.013, ±0.003 and ±0.005 g/cm^3, respectively; the experimental error associated to P_T and P_C was evaluated as ±0.6 and ±0.3%, respectively.

The crystalline fraction, x (wt.%), was also evaluated by density measurements through the expression:

$$x = 100\frac{(1/\rho_g) - (1/\rho_{gc})}{(1/\rho_{g(cr)}) - (1/\rho_{cr})} \quad (5)$$

where ρ_g is the absolute density of parent glass, ρ_{gc} is the absolute density of the glass-ceramic, $\rho_{g(cr)}$ is the density of a hypothetical glass with the composition of the formed crystal phase and ρ_{cr} is the density of the crystal phase. In the case of diopside, it was assumed that ρ_{cr} and $\rho_{g(cr)}$ have values of 3.27 and 2.75 g/cm^3, respectively. The experimental associated error to ρ_g and ρ_{gc} values was evaluated as ±0.003 g/cm^3, to which corresponds an error of ±1% on the evaluation of the crystal phase. A detailed description of the methodological approach used to obtain the relation (5) was reported elsewhere.[23]

The structure and morphology of the crystals in the glass-ceramics were investigated by a Philips XL30CP scanning electron microscopy and back scattering electrons (BSE) observation after polishing and etching the surface for 3 s with 2 wt.% HF solution.

3. Results and discussion

The DTA traces of the three compositions show similar glass transition temperatures, T_g, at about 700 °C, and intensive diopside crystallisation peaks in the interval 850–1000 °C.[22]

The variations, at 5 °C/min heating rate, of apparent and absolute densities of **G1**, **G2** and **G3** glasses as function of the holding temperature, are shown in Figs. 1 and 2, respectively. Figs. 3 and 4 present the percentages of crystal phase formed and the total porosity, obtained by Eqs. (5) and (3), respectively. Similar results were obtained at 20 °C/min heating rate and are reported in Table 2.

In Fig. 1, the densification starts at 700 °C and is completed at 800–850 °C; after 850 °C ρ_a remains constant. Compared to **G1** and **G2**, in **G3** some delay in the densification is observed, probably due to the higher initial porosity of the "green" samples. Figs. 2 and 3 show that the diopside phase formation starts at 750 °C for **G1** and **G2** and at 800 °C for **G3**. Above 900 °C, the amount of crystal phase formed remains constant.

Fig. 4 reports the calculated values, by Eq. (3), of the total porosity. In **G3**, P_T decreases with the temperature up to a minimum constant value after 850 °C. In **G1** and **G2**, the total porosity shows a minimum at 800 °C and than increases.

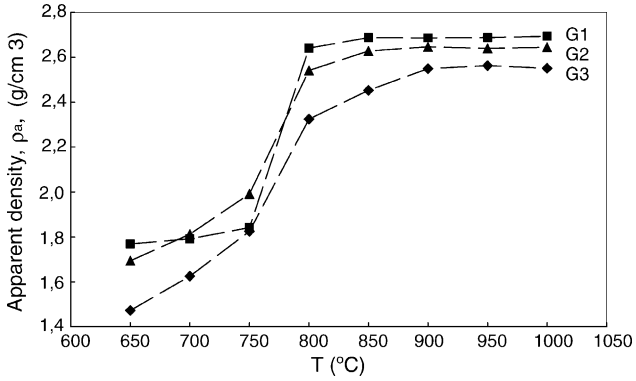

Fig. 1. Variation of the apparent density, ρ_a, of **G1**, **G2** and **G3** at 5 °C/min heating rate, as function of the temperature at 1 h holding.

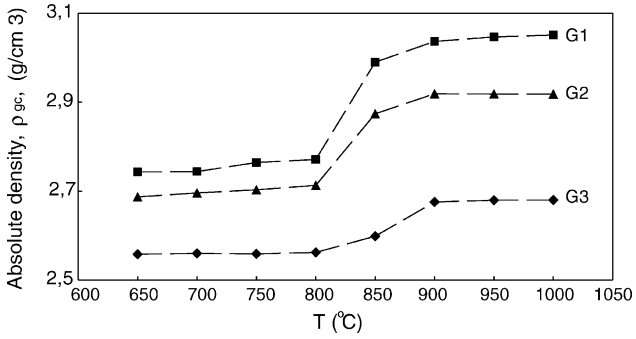

Fig. 2. Variation of the absolute density, ρ_{gc}, of **G1**, **G2** and **G3**, at 5 °C/min heating rate, as function of the temperature at 1 h holding.

The comparison between Figs. 1 and 2 highlights that the sintering ends when begins the formation of diopside crystalline phase, i.e. in the range 800–850 °C. At the same time, by comparing Fig. 3 with Fig. 4 it turns out that after 800 °C the porosity of **G1** and **G2** increases during the crystal phase formation. This series of experimental evidences lead to conclude that the P_T variation, in Fig. 4, cannot be associated to a residual sintering porosity but must be the result of a volume transformation induced by the formation of diopside. In other

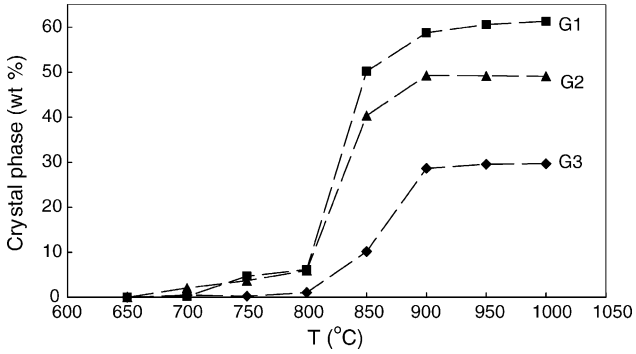

Fig. 3. Variation of the percentage of crystal phase formed (wt.%) of **G1**, **G2** and **G3**, at 5 °C/min heating rate, as function of the temperature at 1 h holding.

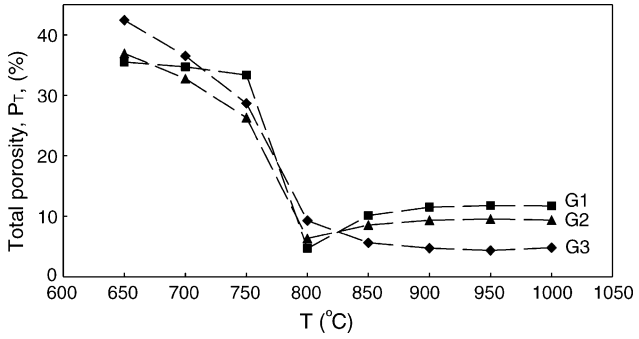

Fig. 4. Variation of the total porosity, P_T, of **G1**, **G2** and **G3**, at 5 °C/min heating rate, as function of the temperature at 1 h holding.

Table 2
Apparent density, ρ_a, and absolute density, ρ_{gc}, of **G1**, **G2** and **G3** at 20 °C/min heating rate

T (°C)	**G1**		**G2**		**G3**	
	ρ_{gc}	ρ_a	ρ_{gc}	ρ_a	ρ_{gc}	ρ_a
650	2.743	1.769	2.687	1.734	2.558	1.473
700	2.743	1.793	2.689	1.822	2.557	1.632
750	2.744	1.847	2.702	2.010	2.557	1.810
800	2.768	2.657	2.709	2.567	2.578	2.289
850	2.983	2.666	2.864	2.632	2.587	2.443
900	3.015	2.678	2.917	2.655	2.668	2.531
950	3.045	2.680	2.922	2.658	2.690	2.537
1000	3.048	2.687	2.922	2.653	2.680	2.531

words, the crystallisation of diopside leads to the formation of a new internal porosity, that will be here named induced crystallisation porosity and labelled as P_{CR}.

The evolution of the porosity, i.e. closed or open, as function of temperature was investigated by measuring the skeleton density. The closed porosity was evaluated by Eq. (4), while the open porosity was calculated as the difference between the total and closed porosity. Fig. 5 shows the variations of open and closed porosity in **G2** composition as function of the temperature, at 5 °C/min heating rate. At low temperatures, up to 750 °C, the porosity is only open, at 800 °C starts the transformation of open porosity into closed, while in the range 850–1000 °C the porosity is practically only closed. By these experiments, which provided similar

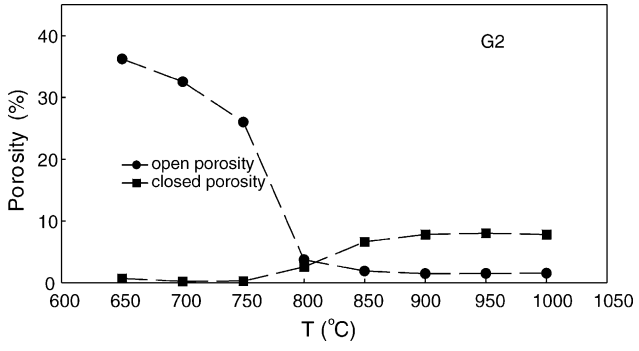

Fig. 5. Variation of the open and closed porosity in **G2**, at 5 °C/min heating rate, as function of the temperature at 1 h holding.

results for **G1** and **G3** (i.e. only closed porosity in the range of 850–1000 °C), it was established that P_{CR} is mainly a closed porosity.

According to the Mackenzie–Shuttleworth model, due to the increasing of the gas pressure in the shrinking closed porous, some residual porosity, P_R, remains in the sintered glass samples.[6] The Mackenzie–Shuttleworth residual porosity, P_R, was evaluated by sintering a non-crystallising SiO_2–CaO–Na_2O glass in the identical experimental conditions of **G1**, **G2** and **G3**. After sintering at 700 °C (i.e. 150 °C higher than T_g), P_R resulted to be $3.6 \pm 0.6\%$. This result is comparable with others obtained in different studies.[9,13]

Assuming the same P_R percentage for **G1**, **G2** and **G3**, the following P_{CR} values are obtained for the samples sintered at 900 °C (i.e. $P_{CR} = P_T - 3.6$): 7.9% in **G1**, 5.7% in **G2** and 1.1% in **G3**. These porosity values, if transformed into percentage of formed diopisde by Eqs. (3) and (5), yield a 47, 33 and 7% for **G1**, **G2** and **G3**, respectively. Taking into account that the total percentage of crystallisation was evaluated as $59 \pm 1\%$, $49 \pm 1\%$ and $30 \pm 1\%$ for **G1**, **G2** and **G3**, respectively, it might be concluded that the volume variation caused by the phase formation is partly transformed into shrinkage of the sample and partly into the formation of induced crystallization porosity in different proportions. The lower is the crystallisation trend of the glass the higher is the shrink of the sample and the lower is P_{CR} formation.

The induced crystallisation porosity was observed by **SEM-BSE**, comparing the imagines of the **G1** polished samples, sintered at 800 and 900 °C for 2 h. In Fig. 6a, the sample held at 800 °C show a sintered grains with residual intergranular porosity and the beginning of surface crystallisation. In Fig. 6b, the sample, sintered at 900 °C shows two types of pores: A, intergranular and similar to the ones observed at 800 °C and B, intragranular and in the centre of the particles, characterised by an intense crystalline formation. In Fig. 7a and b are compared the morphology of the glass ceramic at lower magnification, highlighting the different shapes and dimensions of the residual intergranular and P_{CR} intragranular porosities.

The variation of apparent and absolute densities of **G2-Cr**, obtained at 5 and 20 °C/min, are shown in Figs. 8 and 9, respectively. Figs. 10 and 11 present the percentages of crystal phase formed and the total porosity, respectively.

Fig. 8 demonstrated that by using 5 °C/min heating rate the sintering stops at 800 °C, while by using 20 °C/min at 850 °C. Figs. 9 and 10 show that the diopside formation starts at 700 °C, at 800 °C the percent of crystal phase formed is two times higher than **G2** (see Fig. 3) and at 850 °C the crystallisation process is completed. The bulk crystallisation in **G2-Cr** increases the apparent viscosity and thus inhibits the densification process; as a result, P_T is significantly higher than **G2**. Moreover, as it is shown in Fig. 11, at 5 °C/min the total porosity is higher than at 20 °C/min, which may be related to the better nucleation and higher crystallisation rate induced by the low heating rate. At 5 °C/min heating rate the

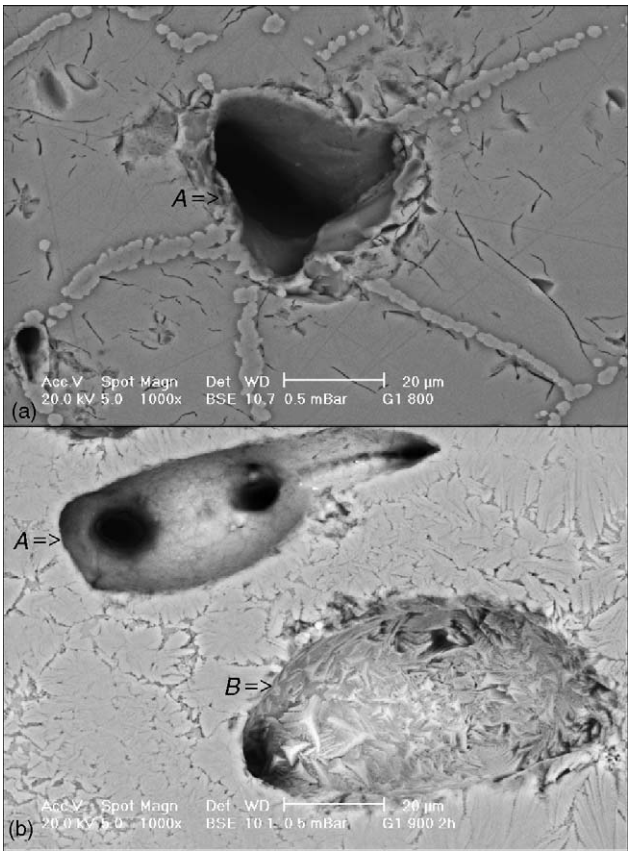

Fig. 6. SEM images of: (a) residual, P_R, pore (labeled A), formed after 2 h isothermal step at 800 °C; (b) residual pore A and induced crystallization pore, P_{CR}, (labeled B) formed after 2 h isothermal step at 900 °C.

total porosity of **G2-Cr** shows a minimum value of 15.3% at 800 °C. Then, due to the intensive diopside formation, P_T increases and at 850 °C becomes 20.4%; the difference of 5.1% may be associated to P_{CR}, corresponding to the formation of 31% diopside. Somewhat similar results were obtained also at 20 °C/min.

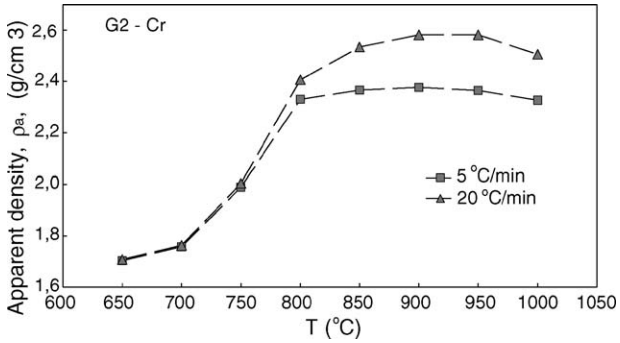

Fig. 8. Variation of the apparent density, ρ_a, of **G2-Cr**, at 5 and 20 °C/min heating rates, as function of the temperature at 1 h holding.

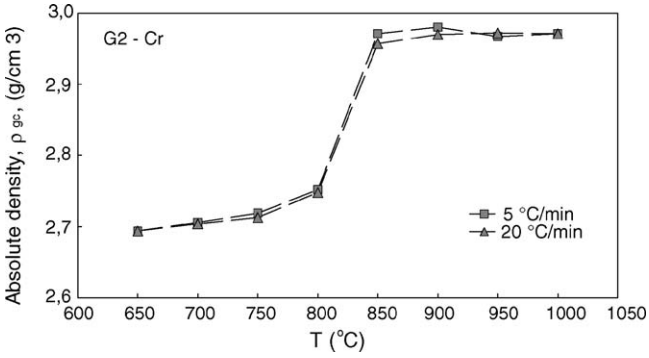

Fig. 9. Variation of the absolute density, ρ_{gc}, of **G2-Cr**, at 5 and 20 °C/min heating rates, as function of the temperature at 1 h holding.

The variation of the open and closed porosity of **G2-Cr** at 5 °C/min as function of the temperature is presented in Fig. 12. The open porosity decreases to 14.5% at 800 °C and then remains constant while the closed porosity starts to increase after 800 °C. The residual open porosity is due to the non completed sintering, while the closed porosity is generated by the diopside crystallisation.

Finally, the crystallisation and the variation of the total porosity as function of time, for **G2** and **G2-Cr**, at 800 °C and

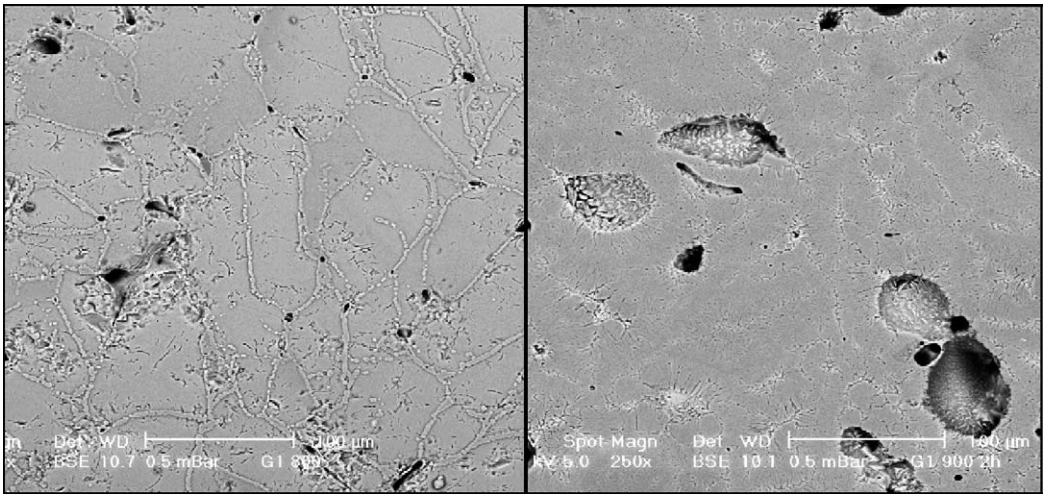

Fig. 7. SEM images of the structure of **G1** samples, after 2 h isothermal step at 800 °C (a) and 900 °C (b).

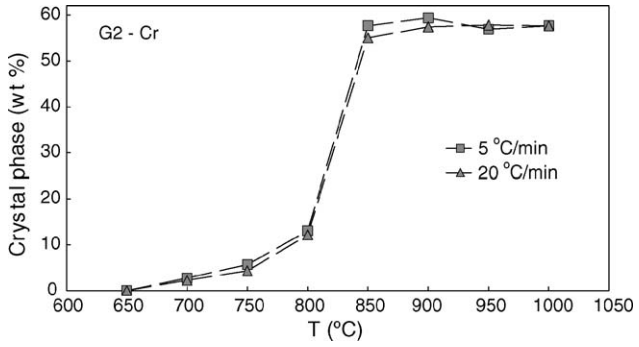

Fig. 10. Variation of the percentage of crystalline phase formed (wt.%) of **G2-Cr**, at 5 and 20 °C/min heating rates, as function of the temperature at 1 h holding.

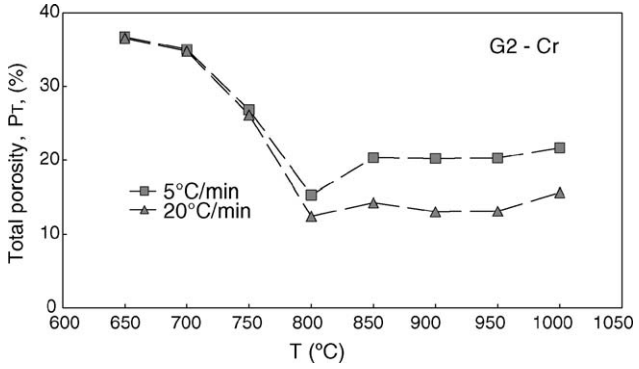

Fig. 11. Variation of the total porosity, P_T, of **G2-Cr**, at 5 and 20 °C/min heating rates, as function of the temperature at 1 h holding.

for times between 1 and 180 min are shown in Figs. 13 and 14, respectively. In **G2**, there is a continuous decrease of P_T up to the minimum value of 3.4% after 120 min; the skeleton density measurements show that this porosity is only closed. Its percentage is similar to the value of 3.6% residual porosity, P_R, evaluated in the non-crystallising SiO_2–CaO–Na_2O glass.

In **G2-Cr**, the densification rate decreases rapidly up to the minimum P_T value of 15.2% obtained after 60 min and 12.5% diopside formation. At this holding time the open and the closed porosites are 14.5 and 0.7%, respectively. After

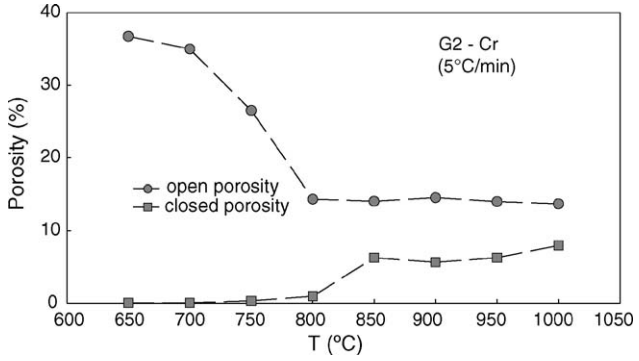

Fig. 12. Variation of the open and closed porosity in **G2-Cr**, at 5 °C/min heating rate, as function of the temperature at 1 h holding.

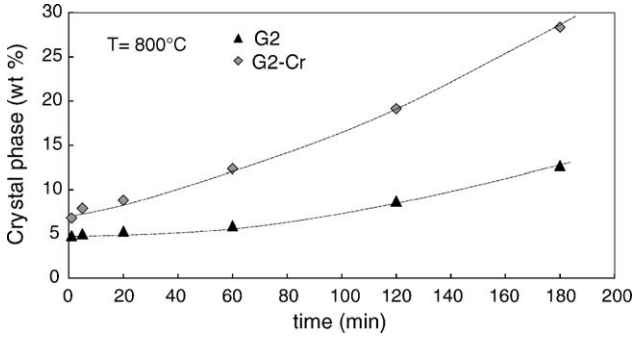

Fig. 13. Variation of the percentage of crystalline phase formed (wt.%) of **G2** and **G2-Cr** as function of the time at 800 °C.

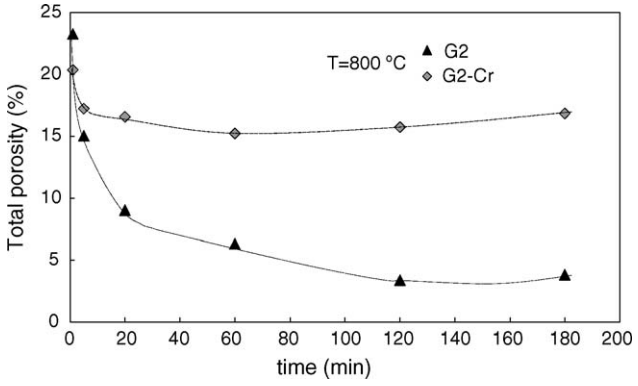

Fig. 14. Variation of the total porosity, P_T, of **G2** and **G2-Cr** as function of the time at 800 °C.

120 min the formed diopside is 28.5%; the open porosity remains constant, while the closed one increases by about 2.5% P_{CR}, corresponding to the 16% diopside formation.

4. Conclusions

The formation of an induced crystallisation porosity, P_{CR}, was shown by applying different pycnometric techniques and was highlighted by SEM-BSE images. This phenomenon may be observed, in the investigated glasses, due to the consistent volume variation connected to the diopside formation in the glassy matrix.

The formation of the P_{CR} increases with the increasing of the crystallisation trend: sintering **G1**, **G2** and **G3** compositions at 900 °C leads to the formation 7.9, 5.7 and 1.1% P_{CR}, respectively; corresponding to 47, 33 and 7% diopside crystallization.

The presence of Cr_2O_3 nucleating agent in **G2** composition, **G2-Cr**, increases the crystallisation and inhibits the sintering; as a result, higher percentage of open porosity is retained in the glass-ceramic. In **G2-Cr**, the densification stops after about 13% diopside formation; the subsequent crystallization leads to the formation of induced crystallization porosity.

A detailed study of the kinetics of P_{CR} formation in **G1** composition will be presented in a next paper.

References

1. Strnad, Z., *Glass-Ceramic Materials*. Elsevier, Amsterdam, 1986.
2. Hőland, W. and Beall, G., *Glass-Ceramics Technology*. The American Ceramics Society, Westerville, 2002.
3. Nakamura S. *Crystallized glass article having a surface pattern*. US Patent 3 955 989, 11.5.1976.
4. Karamanov, A., Gutzow, I. and Penkov, I., Diopside marble-like glass-ceramics. *Glastech. Ber., Glass Sci. Tech.*, 1994, **67**(7), 202–209.
5. Frenkel, J., Viscous flow of crystalline bodies under the action of surface tension. *J. Phys. USSR*, 1945, **9**(5), 385–391.
6. Mackenzie, J. K. and Shuttleworth, R., A phenomenological theory of sintering. *Proc. Phys. Soc. (Lond.), Sec. B*, 1949, **62**, 833.
7. Scherer, G. W., Sintering of low-density glasses: I. *Theory J. Am. Ceram. Soc.*, 1977, **60**(5–6), 236–241.
8. Prado, M. O., Zanotto, E. D. and Müller, R., Model for sintering polydispersed glass particles. *J. Non-Cryst. Solids*, 2001, **279**(2–3), 169–178.
9. Kingery, W. D., Bowen, H. K. and Uhlmann, D. R., *Introduction to Ceramics*. John Willey & Sons, New York, 1975.
10. Hlavac, J., *The Technology of Glass and Ceramics: An Introduction*. Elsevier, Amsterdam, 1983.
11. Müller, R., Kirsh, M. and Lorenz, H., Surface crystallization a limiting effect of sintering glass powders. In *Proceedings of 15th congress on Glass*, *Leningrad*. 1989, **V3**, 334–338.
12. Müller, R., On the kinetics of sintering and crystallization of glass powders. *Glastech. Ber. Glass Sci. Technol.*, 1994, **67C**, 93–99.
13. Zanotto, E. and Prado, M., Isothermal sintering with concurrent crystallisation of monodispersed and polydispersed glass particles. Part 1. *Phys. Chem. Glasses*, 2001, **42**(3), 191–198.
14. Karamanov, A., Penkov, I. and Gutzow, I., *A new marble-like sintered glass-ceramic material. Fundamentals of Glass Sciences and Technology*. ESG, Venice, Italy, 1993, pp. 675–679.
15. Gutzow, I., Paskova, R., Karamanov, A. and Schmelzer, J., The kinetics of surface induced sinter-crystallization and the formation of glass-ceramic materials. *J. Mater. Sci.*, 1998, **33**(21), 5265–5273.
16. Krieger, I. M., Rheology of monodispersed latices. *Adv. Colloid Interface Sci.*, 1972, **3**, 111–117.
17. Reed, J. S., *Principles of Ceramic Proceedings* (*2nd ed.*). Jon Wiley & Sons, New York, 1995.
18. Fan, Z. and Boccaccini, A. R., A new approach to the effective viscosity of suspension. *J. Mater. Sci.*, 1996, **31**, 2515–2521.
19. Ryu, B. and Yasui, I., Sintering and crystallization behavior of a glass powder and bloks with a composition of anorthite and the microstructure dependence of its thermal expansion. *J. Mater. Sci.*, 1994, **29**, 3323–3328.
20. Pascual, M. J., Duran, A. and Pascual, L., Sintering process of glasses in the system Na_2O–B_2O_3–SiO_2. *J. Non-Cryst. Solids*, 2002, **306**, 58–69.
21. Schairer, J. F. and Yoder Jr., H. S., Nature of residual liquids from crystallization, with data on the system nepheline–diopside silica. *Am. J. Sci.* 1960, **258A**, 273–283 (Bradley volume).
22. Karamanov, A., Arrizza, L., Matecovetc, I. and Pelino, M., Properties of sintering glass-ceramics belonging to the system diopside–albite. *Ceram Int*, 2004, **30**, 2129–2135.
23. Karamanov, A. and Pelino, M., Evaluation of the degree of crystallisation in glass-ceramics by density measurements. *J. Eur. Ceram. Soc.*, 1999, **19**(5), 649–654.
24. Zanotto, E. D. and Muler, E. A., A simple method to predict the nucleation mechanism in glass. *J. Non-Cryst. Solids*, 1991, **130**, 220–221 (Letter to the Editor).
25. Schmelzer, J., Moller, J., Gutzow, I., Pascova, R., Müller, R. and Pannhorst, W., Surface energy and structure effects on surface crystallization. *J. Non-Cryst. Solids*, 1995, **183**, 215–223.
26. Rawlings, R. D., Production and properties of silceram glass-ceramic, in glass-ceramic materials—fundamentals and applications. *Series of Monographs on Material Science*, *Engineering and Technology*. Mucchi Editore, 1997, pp. 115–133.
27. Karamanov, A., Pisciella, P. and Pelino, M., The effect of Cr_2O_3 as nucleating agent in iron rich glass-ceramics. *J. Eur. Ceram. Soc.*, 1999, **19**(15), 2641–2645.
28. Rezvani, M., Eftekhari-Yekta, B., Solati-Hashjin, M. and Marghussian, V. K., Effect of Cr_2O_3, Fe_2O_3 and TiO_2 nucleants on the crystallization behaviour of SiO_2–Al_2O_3–CaO–MgO(R_2O) glass-ceramics. *Ceram. Int.*, 2005, **32**, 75–80.